Statistical Properties of InterParticle/Void Distance for Amorphous Plastics Toughening

Nam Ho Kim, Ho Sung Kim

Mechanical Engineering, School of Engineering, Faculty of Engineering and Built Environment, University of Newcastle, Callaghan, NSW 2308, Australia

Received 18 May 2005; accepted 8 September 2005
DOI 10.1002/app.23172
Published online in Wiley InterScience (www.interscience.wiley.com).

ABSTRACT: Statistical properties of interparticle/void distance (ID) for various particle/void and dispersion types are studied in relation with toughening of plastics using computer-generated three-dimensional models. Particle/void size groups adopted were either of constant diameter or of log-normal distribution. Particles/voids were dispersed at uniform-random or flocculated with multiple clusters. It was found that IDs are (a) of approximately Gaussian distribution for particles/voids of either a constant diameter or a log-normal distribution, when they are dispersed at uniform-random, but (b) not of Gaussian distribution for particle/void sizes of bimodal log-normal distribution, nor for flocculated log-normal distribution of particles/voids dispersed with multiple clusters. It was also found that the degree of ID uniformity for a single group of log-normally sized particles/voids is not sensitive to standard deviation of particle/void size. Mixing effect on ID properties using two groups of log-normally distributed particles/voids with similar mean particle/void diameters was simulated. It was found that, when a significant amount (36 vol %) of particles/voids of a small mean and standard deviation of ID was mixed with a group of particles/voids of a large mean and standard deviation of ID, mean and standard deviation of ID for the mixture were not substantially lower than those of the group of particles/voids of the large mean and standard deviation of ID. It was also found that the degree of ID uniformity for the mixture of the two groups was lower than those of individual groups, indicating that the mixing has deleterious effect on toughening. J Appl Polym Sci 101: 4256–4262, 2006

Key words: toughness; particle size distribution; dispersions; fracture; mixing; interparticle/void distance; particulate composite

INTRODUCTION

Brittle polymers have been modified for high toughness. Toughening can be achieved by the addition of particles/voids.[1–5] One of the important parameters for toughening has been found to be the surface-to-surface interparticle/void distance (ID) (or ligament length between particles/voids), since Wu[6,7] first suggested. The reason for this is that a localized microscopic plane stress–strain deformation transition between particles/voids generally depends on ID. Also, in the case of semicrystalline polymers, preferably oriented crystalline layers form around particles and the layer thickness affects the critical ID.[2,8]

In general, toughness of a particulate composite is dependent upon properties of particles, of interface between particles and matrix, and of matrix. Matrix deformation would become large when subjected to stresses, as interface bonding strength and particle elastic modulus (generally properties) decrease. The interface bonding is usually ill defined because of the difficulty of the small-scale characterization, although interlayer between particle and matrix can be introduced by coating.[9] Examples for high and low ends of the spectrum of elastic modulus, though, may be glass beads[10–12] and rubber, respectively. Rubber has been used for both thermosets and thermoplastics, owing to its remarkable toughening effect, since early years.[6,13] Microtoughening mechanisms of thermosets have well been characterized. Pearson and Yee[14] suggested that major toughening mechanisms are cavitation and shear deformation of matrix between rubber particles. Bagheri and Pearson[15,16] supported the shear deformation as the major toughening mechanism and elucidated the role of cavitation itself of particles using hollow microspheres. Further, Kim and Kim[5] employed voids for toughening of epoxy, where toughening is entirely dependent on properties of matrix and found that shear deformation between voids is also a major toughening mechanism. At the same time, they demonstrated that the toughening is related to a critical ID.

Wu[7] has already indicated that flocculation has deleterious effect on toughening, because the matrix deformation tends to be localized as flocculation level

Correspondence to: H. S. Kim (ho-sung.kim@newcastle.edu.au).

Contract grant sponsor: University of Newcastle (RGC project grant).

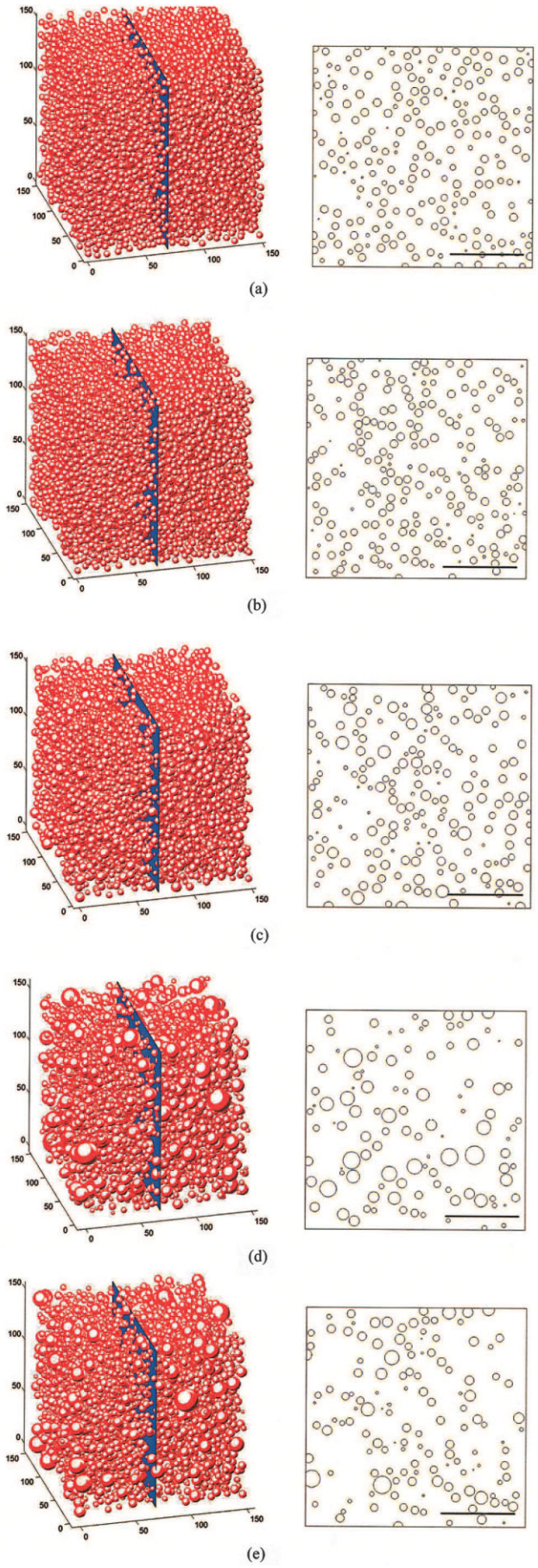

increases and it would not propagate if the degree of flocculation is high. Thus, it is important to maintain ID uniformity for plastics toughening involving, particularly, shear banding between particles/voids. Recently, Kim and Kim[17] suggested a new practical method for measuring the flocculation (or ID uniformity) as well as ID, since the relationship of ID with various parameters suggested by Wu[7] is only for ideal arrays of particles. In this paper, the effect of particle/void size distribution on ID distributions for various types of particle/void dispersions are investigated using computer-generated particles/voids and the new ID measuring method.[17]

PARTICLE/VOID GENERATION

3D models for six different types were computer generated (using MATLAB 6.5) by varying particle/void size and dispersion, and then cross sections were obtained as shown in Figures 1 and 2. Statistical properties of generated particles/voids are summarized in Table I. The first five types (Fig. 1) are for a constant volume fraction of 0.15. The first two types (Type I and Type II—Figs. 1(a) and 1(b)) are both of monosized particles/voids with a diameter (d_p) of 5.35 μm but of different minimum interparticle/void distances. The minimum interparticle/void distances nominated for Type I and Type II (Figs. 1(a) and 1(b)) were 1.5 μm and zero, respectively, during random number generation. Type III and Type IV (Figs. 1(c) and 1(d)) are of log-normally sized particles/voids randomly generated using

$$r_p = \exp[r_i] \tag{1}$$

where r_i is the radius of Gaussian distribution. The log-normal distribution is common in particle distribution.[6] A mean of 1 (mean diameter ($=\bar{d}_p$) = 5.44 μm) was nominated for r_i of both Type III and Type IV

Figure 1 Computer-generated 3D models with cross sections for randomly distributed particles/voids with a volume fraction of 0.15. (a) Monosized particles/voids of 5.35 μm in diameter and a minimum interparticle/void distance of 1.5 μm; (b) monosized particles/voids of 5.3 μm in diameter and a minimum interparticle/void distance of zero; (c) log-normally sized particles/voids with a mean of 5.57 μm and a standard deviation of 1.13 μm; (d) log-normally sized particles/voids with a mean of 5.91 μm and a standard deviation of 2.46 μm; and (e) log-normally sized bimodal particles/voids with a similar mean particle/void size of 5.74 μm but different standard deviations of 1.11 and 2.47 μm, and respectively, volume fractions of 0.054 and 0.096. The location of each cross section is shown on 3D model. The scale bar on the cross section represents 50 μm. [Color figure can be viewed in the online issue, which is available at www.interscience.wiley.com.]

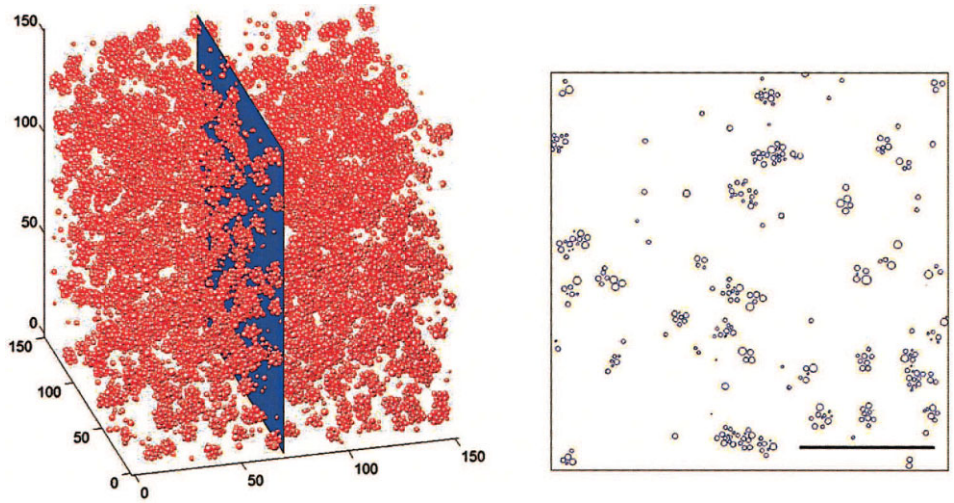

Figure 2 Computer-generated 3D image of randomly distributed particles/voids and its cross section for a volume fraction of 0.03. Particle/void mean size = 1.22 μm, number of clusters = 3000, standard deviation for distance from each cluster center = 1, and minimum cluster center distance = 3 μm. The scale bar represents 50 μm. [Color figure can be viewed in the online issue, which is available at www.interscience.wiley.com.]

(Figs. 1(c) and 1(d)), and respectively, standard deviations of 0.2 and 0.4 were also nominated for r_i.

Type V is of also log-normally sized particles/voids and bimodal size distribution. It is a type of combination of Type III and Type IV, with the same nominated mean particle/void radius ($\bar{r}_i$) with standard deviations (for r_i) of 0.2 and 0.4 respectively, and volume fractions of 0.054 and 0.096 respectively.

Type VI (Fig. 2) is of flocculated dispersion with a log-normally sized mean particle/void of 0 for r_i (d_p = 2.00 μm) and a volume fraction of 0.03. It was generated by producing 3000 random cluster centers, with a minimum distance (MD) of 3 μm between cluster centers, and then particles/voids were placed around the cluster centers. The particle/void distances from each center were of Gaussian distribution with a standard deviation of 1.

PROCEDURE FOR 2D INTERPARTICLE/VOID DISTANCE MEASUREMENTS

The following procedure[17] was adopted for measuring IDs of particle/void dispersion on the cross sections (Figs. 1 and 2).

1. Nominate an arbitrary particle/void for commencement (e.g., particle/void '1' in Fig. 3).
2. Choose a nearest particle/void (e.g., particle/void '2' in Fig. 3) to the first nominated particle/void and then draw a connecting line between two surfaces of particles/voids.
3. Choose another particle/void (e.g., particle/void '3' in Fig. 3) which is the nearest to the midpoint between previous two particle/void surfaces.
4. Draw a triangle connecting previous two particle/void surfaces.

TABLE I
Statistics for Particle/Void Size and ID

	Particle/void					ID			
Type	Measured mean of diameter (μm) ($\bar{d}_p$)	Measured standard deviation (μm) (σ_p)	3D Particle/void total numbers generated	Minimum distance between particles/voids	Volume fraction	Arithmetic mean (μm) $\overline{ID}$	Arithmetic standard deviation (σ_{ID})	Numbers	Coefficient of variation (CV)
I	5.35	0	6329	1.5	0.15	7.44	3.94	626	0.53
II	5.35	0	6329	0	0.15	7.32	4.55	606	0.61
III	5.57	1.13	4996	0	0.15	7.98	4.60	519	0.58
IV	5.91	2.46	2904	0	0.15	10.95	6.56	280	0.60
V	5.74	1.93 (1.11/2.47)	1823/1824	0	0.15 (0.054/0.096)	10.08	6.50	364	0.64
VI	2.04	0.42	20103	0	0.03	7.71	9.48	766	1.23

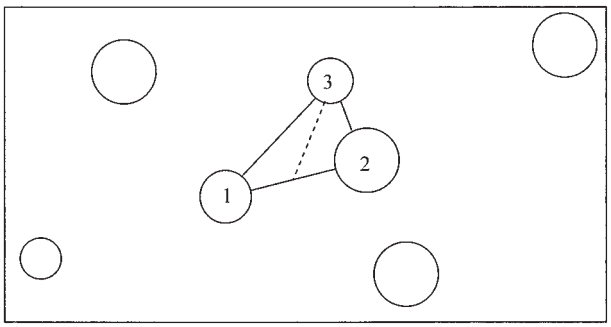

Figure 3 Schematic particle/void dispersion and line connection. The numbering indicates the order of choice for connection.

5. Repeat steps 3 and 4 using one of the unused and outermost line(s) of triangle(s) until all the particles/voids are connected.
6. Remove all the lines affected by the edges of 2D image outline (see Appendix).
7. Finally measure interparticle/void distances.

IDs were measured using an image analyzer, Scion Image.

RESULTS AND DISCUSSION

Statistical properties of ID measurements for various types of particle size distribution randomly dispersed are given in Figure 4 and for flocculated dispersion in Figure 5. Summary statistics for IDs are listed in Table I. The normalized ID (Fig. 4) is given by

$$\frac{\mathrm{ID} - \overline{\mathrm{ID}}}{\sigma_{\mathrm{ID}}} \tag{2}$$

where σ_{ID} is the ID standard deviation and $\overline{\mathrm{ID}}$ is the (arithmetic) ID mean. The cumulative frequency curve (F(ID) in Fig. 4 is based on the Gaussian distribution given by

$$F(\mathrm{ID}) = \frac{1}{\sigma_{\mathrm{ID}}\sqrt{2\pi}} \int_{-\infty}^{\mathrm{ID}} \exp\left[\frac{-(\mathrm{ID} - \overline{\mathrm{ID}})^2}{2(\sigma_{\mathrm{ID}})^2}\right] d(\mathrm{ID}) \tag{3}$$

Type I (Fig. 1(a)) usually occurs in precipitated particle dispersion. In this case, no particles are in contact and the MD between particles would depend on man-

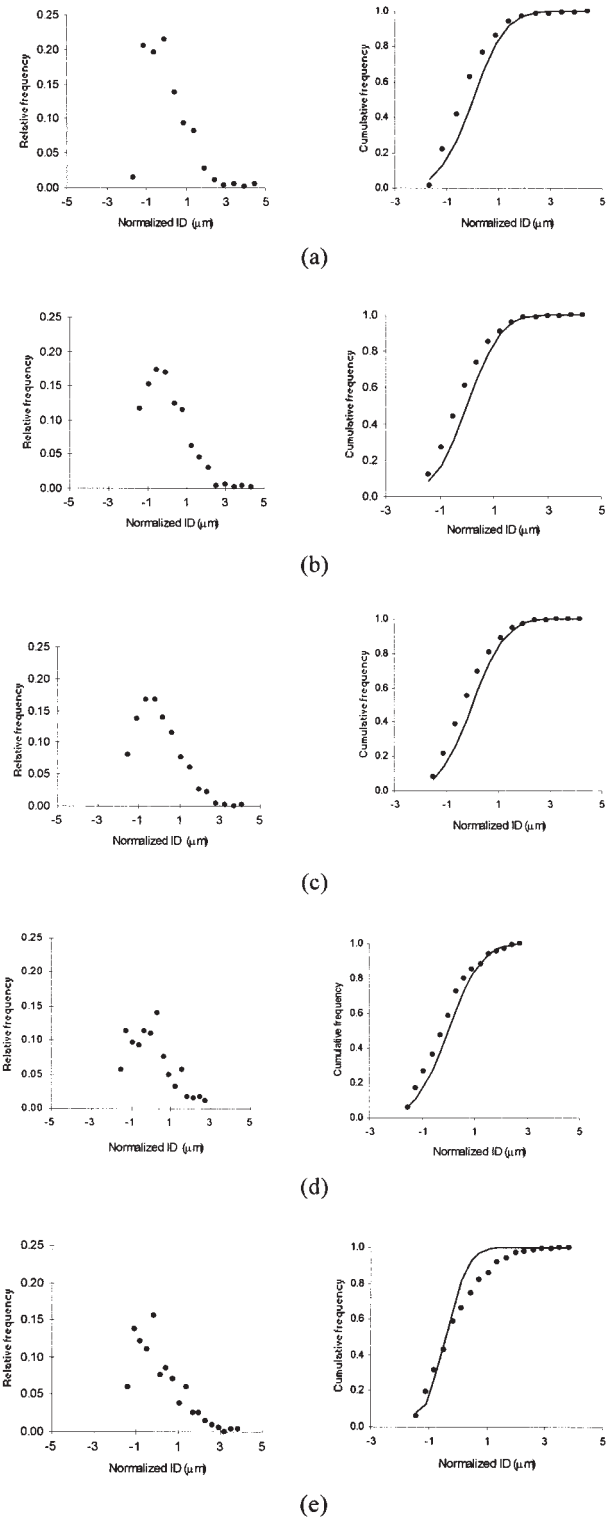

Figure 4 Relative and cumulative frequencies as a function of normalized ID. (a) Type I, monosized particles/voids of 5.35 μm and a minimum interparticle/void distance of 1.5 μm; (b) Type II monosized particles/voids of 5.35 μm and a minimum interparticle/void distance of zero; (c) Type III, log-normally sized particles/voids with a mean of 5.57 μm and a standard deviation of 1.13 μm; (d) Type IV, log-normally sized particles/voids with a mean of 5.91 μm and a standard deviation of 2.46 μm; and (e) Type V, log-normally sized bimodal particles/voids with a similar mean particle/void size of 5.74 μm but different standard deviations of 1.11 and 2.47 μm, and respectively, volume fractions of 0.096 and 0.054. The curves represent cumulative Gaussian distribution functions.

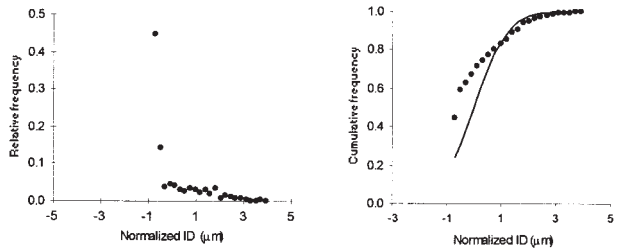

Figure 5 Relative and cumulative frequencies as a function of normalized ID for flocculated dispersion. The curve represents cumulative Gaussian distribution function.

ufacturing conditions. Type I dispersion can be compared with that of real precipitated CTBN rubber particles as shown in Figure 6 (sourced from ref.[18]), without considering particle size distribution type. All other types (Figs. 1(b)–1(e)) are the cases where MD is zero, which occurs for preformed particle dispersions. They can be also compared with a real preformed particle dispersion shown in Figure 7 (sourced from ref.[19]). The computer-generated dispersions generally appear to be visually compatible with real dispersions. Type I and Type II (Figs. 1(a) and 1(b)) were to simulate the effect on ID of MD between particles/voids. If the MD increases, the degree of ID uniformity, which can be represented by the inverse of the coefficient of variation (1/CV), would increase and approach the ideal dispersion of ID. When the MD is zero (as in Type II), the degree of ID uniformity is relatively low as expected compared with that of Type I (Fig. 1). Both σ_{ID} and CV for Type II (Fig. 1(b)) are 15% larger than those of Type I (Fig. 1(a)). It is thus confirmed that ID standard deviation (σ_{ID}) is a good indicator for flocculation for a given group of particles/voids—the higher σ_{ID}, the more flocculation, as demonstrated previously.[17] Also, it indicates that precipitated particle dispersion is usually superior to preformed particle dispersion in toughening. The normalized cumulative frequency (Fig. 4), in the mean time, appears to be of approximate Gaussian distribution for both Type I and Type II.

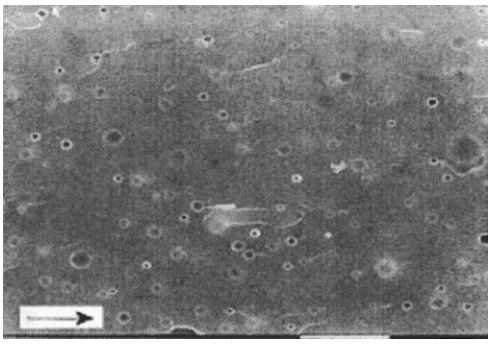

Figure 6 SEM image of fracture surface showing precipitated rubber particles of 4 phr.

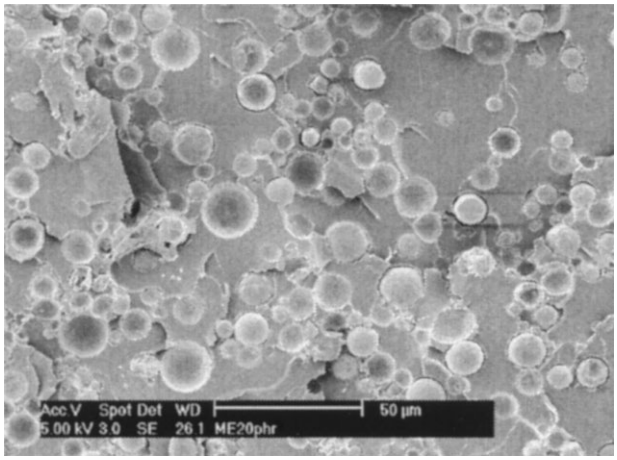

Figure 7 SEM image of fracture surface showing preformed plastic particles of 20 phr.

Types III and IV were to simulate the effect of σ_p on ID. Both mean ($\overline{ID}$) and standard deviation (σ_{ID}) are found to be substantially increased with increasing σ_p (Table I)—37% in $\overline{ID}$ and 43% in σ_{ID} for 118% increase in σ_p. The reason for this appears that, as σ_p increases, the volume of particles/voids whose diameters are larger than $\bar{d}_p$ increases, and these ones contribute to reduction in particle/void numbers, resulting in increase in both $\overline{ID}$ and σ_{ID}, as visualized in Figures 1(c) and 1(d). It is noticed, however, that the degree of ID uniformity (1/CV) is not sensitive to the variation of σ_p. It should be noted that a high degree of ID uniformity is desired for plastics toughening. Also, the normalized cumulative frequencies for IDs (Figs. 4(c) and 4(d)) still appear to follow approximately the Gaussian distribution irrespective of σ_p variation.

Type V (Fig. 1(e)) was to simulate mixing of particles/voids from Type III and Type IV. As expected, $\overline{ID}$ and σ_{ID} of Type V lie between Type III and Type IV (Table I). It is noted, though, that there is not much difference between those of Type IV and Type V, although volume fraction of Type III (36%) is significantly high. This indicates that the mixing does not substantially improve $\overline{ID}$ and σ_{ID}. Further, the mixing of two different groups raises the CV (= 0.64) of the combined group (Type V), so that its degree of ID uniformity is not higher than those (CV = 0.58 and 0.60) of individual groups. This indicates that the mixing has deleterious effect on toughening. This information can be important for practical applications. Also, it is interesting to find that the normalized cumulative frequency of Type V (Fig. 4(e)) for IDs no longer follows the Gaussian distribution. It begins to deviate from the Gaussian distribution at about 0.6 in frequency.

Type VI (Fig. 2) is strongly flocculated, possessing multiple identifiable clusters, compared to all other dispersion types. Statistical parameters of this type are

not directly comparable with those of other types, because they were generated with different way of particle/void generation, although particle/void sizes are log-normally distributed. However, given that $\overline{ID}$s of Type I, Type II, and Type III are similar to that of Type VI, it is noted that σ_{ID} of Type VI is very large compared to those of other types of dispersion (Table I). The normalized cumulative frequency for ID (Fig. 5) is seen to be far from the Gaussian distribution.

CONCLUSIONS

Statistical properties of interparticle/void distance (ID) for various types of dispersion and size distribution of particles/voids have been studied. It has been found that IDs are

a. Approximately of Gaussian distribution for particles/voids of either a constant diameter or a log-normal distribution when they are dispersed at uniform-random; but,
b. not of Gaussian distribution for particle/void sizes of bimodal log-normal distribution (mixture of two groups) nor for flocculated log-normal distribution of particles/voids dispersed with multiple clusters.

Also, it has been found that the degree of ID uniformity, which can be represented by the inverse of the coefficient of variation, for a single group of log-normally sized particles/voids is not sensitive to the standard deviation of particle/void size (σ_p). This finding coincided with IDs being of approximate Gaussian distribution.

Mixing effect on ID properties using two groups of log-normally distributed particles/voids with similar mean particle/void diameters has been simulated. It has been found that, when a significant amount (36 vol %) of particles/voids of a small $\overline{ID}$ and σ_{ID} were mixed with a group of particles/voids of a large $\overline{ID}$ and σ_{ID}, $\overline{ID}$ and σ_{ID} of the mixture were not substantially lower than those of the group of particles/voids of a large $\overline{ID}$ and σ_{ID}. This indicates that the mixing does not substantially improve ID properties of the particle/void group of a large $\overline{ID}$ and σ_{ID}. It has also been found that the degree of ID uniformity for the mixture of the two particle/void groups are lower than those of individual groups, indicating that the mixing has deleterious effect on toughening.

APPENDIX

False particle/void distance due to edge effect, and methods for removal

As the triangulation progresses, according to the procedure (see Procedure for 2D Interparticle/Void Distance Measurements section), toward edges of 2D image box, some false particle/void distance lines are formed. The false lines are due to the shortage of particle/void choices along the edges when step 3 in the procedure is implemented, resulting in choice of particle/void which is located sideways from the mid-point rather than the particle/void forward. The false lines, therefore, tend to be longer than the true distances. An example is given in Figure A1, where an image is taken from the middle part of a cross section (Fig. A1(a)), and triangulation on it is completed as shown in Figure A1(b). The difference in line length is seen along the edges between the two images.

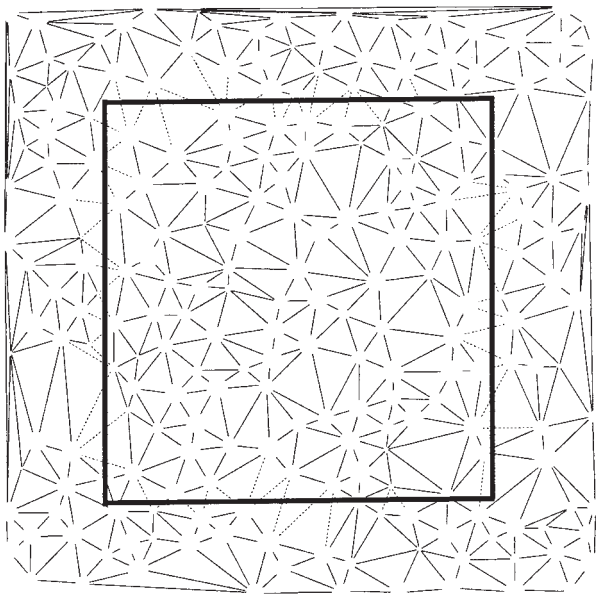

(a)

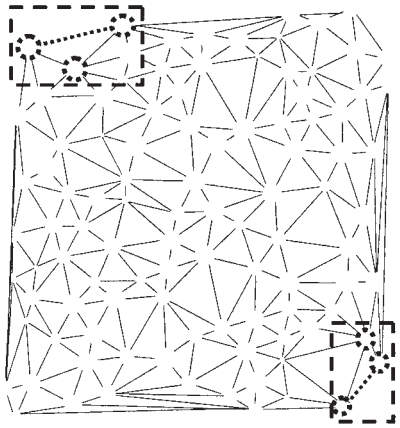

(b)

Figure A1 Triangulation and ID: (a) a cross section showing IDs after triangulation and (b) square section taken from (a) showing false IDs along the edge after retriangulation.

To remove such lines representing false IDs, the outermost perimeter of the triangulation network can be started to be removed until the mean line length becomes flat in a plot of mean interparticle/void distance *versus* number of outer perimeters. In this method,[17] even some lines representing true IDs can be unnecessarily removed. In the current method, each triangle was selected from the outermost layer of triangles first, and then next layer and so on for determining whether an ID line forming part of outermost perimeter of lines should remain or be deleted. The following procedure for the determination is developed (see Fig. A2):

1. Two tangent lines to two circles (representing voids/particles) at the two ends of each inner ID line (note two inner ID lines are available in one triangle at the commencement but only one inner ID line is sometimes available afterwards) are drawn outwards.
2. If there is no void/particle between the two tangent lines of each inner ID line, the subject ID line is to be deleted or otherwise retained.

An example is given in Figure A3, showing triangulation after removing lines representing false ID using the sample given in Figure A1(b). It is found that the resulting triangulation is very similar to the one in inner box in Figure A1(a).

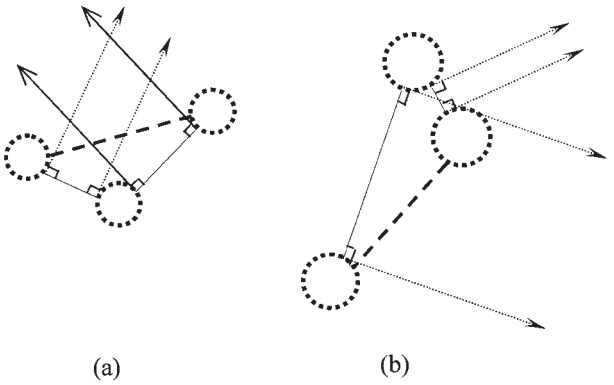

Figure A2 Examples taken from Figure A1(b) for determining whether an ID line forming part of outermost perimeter of lines should remain or be deleted. Dashed connecting lines are part of the outermost perimeter of lines whereas solid lines are inner ID lines. (a) dashed line to be deleted and (b) dashed line to remain.

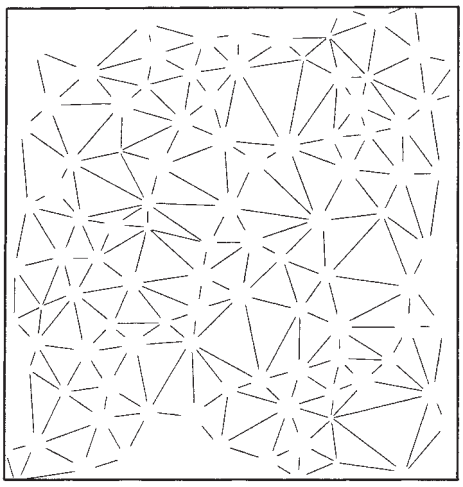

Figure A3 Triangulation after removing lines representing false IDs using the sample given in Figure A1(b).

One of us (NHK) gratefully acknowledges the UNRS scholarship provided by the University of Newcastle.

References

1. Bucknall, C. B. Toughened Plastics; Applied Science Publications: London, 1977.
2. Bartczak, Z.; Argon, A. S.; Cohen, R. E.; Weinberg, M. Polymer 1999, 40, 2331.
3. Waddil, H. G. Presented at the 11th National SAMPE technical Conference, Boston, November 13–15, 1979. p 282.
4. Huang, Y.; Kinloch, A. J. Polymer 1992, 92, 1330.
5. Kim, N. H.; Kim, H. S. J Appl Polym Sci, 2005, 98, 1290.
6. Wu, S. Polymer 1985, 26, 1855.
7. Wu, S. J Appl Polym Sci 1988, 35, 549.
8. Arostegui, A.; Nazabal, J. Polymer 2003, 44, 5227.
9. Amdouni, N.; Sautereau, H.; Gerard, J. F.; Fernagut, F.; Coulon, G.; Lefebvre, J. M. J Mater Sci 1990, 25, 1435.
10. Lee, J.; Yee, A. F. Polymer 2000, 41, 8363.
11. Lee, J.; Yee, A. F. Polymer 2001, 42, 577.
12. Lee, J.; Yee, A. F. Polymer 2001, 42, 589.
13. Sultan, J. N.; McGarry, F. J. J Appl Polym Sci 1973, 13, 29.
14. Pearson, R. A.; Yee, A. F. J Mater Sci 1986, 21, 2475.
15. Bagheri, R.; Pearson, R. A. Polymer 1995, 36, 4883.
16. Bagheri, R.; Pearson, R. A. Polymer 1996, 37, 4529.
17. Kim, N. H.; Kim, H. S. Scr Mater 2005, 52, 739.
18. Kim, H. S.; Ma, P. J Appl Polym Sci 1996, 61, 659.
19. Kim, N. H.; Kim, H. S. J Appl Polym Sci, 2005, 98, 1663.